SHIP PRODUCTION COMMITTEE
FACILITIES AND ENVIRONMENTAL EFFECTS
SURFACE PREPARATION AND COATINGS
DESIGN/PRODUCTION INTEGRATION
HUMAN RESOURCE INNOVATION
MARINE INDUSTRY STANDARDS
WELDING
INDUSTRIAL ENGINEERING
EDUCATION AND TRAINING

November 1993
NSRP 0408

THE NATIONAL SHIPBUILDING RESEARCH PROGRAM

1993 Ship Production Symposium

Paper No. 25: Measured Imperfections and Their Effects on Strength of Component Plates of a Prototype Hull Structure

U.S. DEPARTMENT OF THE NAVY
CARDEROCK DIVISION,
NAVAL SURFACE WARFARE CENTER

Report Documentation Page

Form Approved
OMB No. 0704-0188

Public reporting burden for the collection of information is estimated to average 1 hour per response, including the time for reviewing instructions, searching existing data sources, gathering and maintaining the data needed, and completing and reviewing the collection of information. Send comments regarding this burden estimate or any other aspect of this collection of information, including suggestions for reducing this burden, to Washington Headquarters Services, Directorate for Information Operations and Reports, 1215 Jefferson Davis Highway, Suite 1204, Arlington VA 22202-4302. Respondents should be aware that notwithstanding any other provision of law, no person shall be subject to a penalty for failing to comply with a collection of information if it does not display a currently valid OMB control number.

1. REPORT DATE	2. REPORT TYPE	3. DATES COVERED
NOV 1993	**N/A**	**-**

4. TITLE AND SUBTITLE	5a. CONTRACT NUMBER
The National Shipbuilding Research Program 1993 Ship Production Symposium Paper No. 25: Measured Imperfections and Their Effects on Strength of Component Plates of a Prototype Hull Structure	5b. GRANT NUMBER
	5c. PROGRAM ELEMENT NUMBER
6. AUTHOR(S)	5d. PROJECT NUMBER
	5e. TASK NUMBER
	5f. WORK UNIT NUMBER
7. PERFORMING ORGANIZATION NAME(S) AND ADDRESS(ES) **Naval Surface Warfare Center CD Code 2230 - Design Integration Tower Bldg 192 Room 128 9500 MacArthur Blvd Bethesda, MD 20817-5700**	8. PERFORMING ORGANIZATION REPORT NUMBER
9. SPONSORING/MONITORING AGENCY NAME(S) AND ADDRESS(ES)	10. SPONSOR/MONITOR'S ACRONYM(S)
	11. SPONSOR/MONITOR'S REPORT NUMBER(S)

12. DISTRIBUTION/AVAILABILITY STATEMENT
Approved for public release, distribution unlimited

13. SUPPLEMENTARY NOTES

14. ABSTRACT

15. SUBJECT TERMS

16. SECURITY CLASSIFICATION OF:			17. LIMITATION OF ABSTRACT	18. NUMBER OF PAGES	19a. NAME OF RESPONSIBLE PERSON
a. REPORT	b. ABSTRACT	c. THIS PAGE			
unclassified	**unclassified**	**unclassified**	**SAR**	**14**	

Standard Form 298 (Rev. 8-98)
Prescribed by ANSI Std Z39-18

DISCLAIMER

These reports were prepared as an account of government-sponsored work. Neither the United States, nor the United States Navy, nor any person acting on behalf of the United States Navy (A) makes any warranty or representation, expressed or implied, with respect to the accuracy, completeness or usefulness of the information contained in this report/ manual, or that the use of any information, apparatus, method, or process disclosed in this report may not infringe privately owned rights; or (B) assumes any liabilities with respect to the use of or for damages resulting from the use of any information, apparatus, method, or process disclosed in the report. As used in the above, “Persons acting on behalf of the United States Navy” includes any employee, contractor, or subcontractor to the contractor of the United States Navy to the extent that such employee, contractor, or subcontractor to the contractor prepares, handles, or distributes, or provides access to any information pursuant to his employment or contract or subcontract to the contractor with the United States Navy. ANY POSSIBLE IMPLIED WARRANTIES OF MERCHANTABILITY AND/OR FITNESS FOR PURPOSE ARE SPECIFICALLY DISCLAIMED.

0408

THE NATIONAL SHIPBUILDING RESEARCH PROGRAM

1993

SHIP PRODUCTION SYMPOSIUM

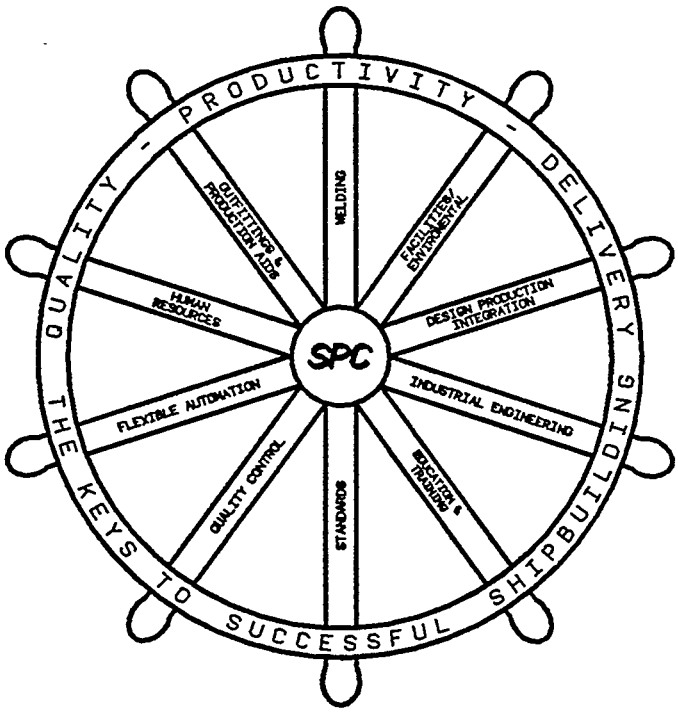

Sponsored by the Hampton Roads Section
Society of Naval Architects & Marine Engineers

CENTENNIAL
1893-1993

Williamsburg Virginia, November 1-4, 1993

CENTENNIAL
1893-1993

The National Shipbuilding Research Program
1993 Ship Production Symposium
Sponsored by the Hampton Roads Section SNAME

Measured Imperfections and Their Effects on Strength of Component Plates of A Prototype Double Hull Structure

Alan AhKum Pang (V), Robert Tiberi (V), Le Wu Lu (V), James Ricles (V) and
Robert Dexter (V) -Lehigh University, PA.

ABSTRACT

The U.S. Navy is currently studying the use of double hull designs in high strength low alloy (HSLA) steels for surface combatant ships. A full scale prototype double hull module was fabricated, from which multicellular box column specimens were cut for compressive tests to failure. Initial imperfections, i.e., initial plate deflections and welding residual stresses, affect the stiffness and strength of welded members. This paper describes the measurement of these imperfections and the analysis of their effects on the component plates of the cellular box specimens. Initial deflections were measured in the laboratory, where the maximum values did not exceed the Navy's guidelines or proposed values of several researchers. Residual stresses in a box specimen were also measured in the laboratory under more controlled conditions. Using the measured imperfections, the plate arrangements were analyzed using the finite element method. The imperfections were found to reduce the stiffness and strength of the plates. The results showed that for accurate prediction of the strength of welded plates, initial imperfections must be taken into account.

INTRODUCTION

Many double hull ship designs consist of twin skins of plating wrapping around the ship bottom, sides and, optionally, the main deck. The nearly parallel plates are separated and stiffened by longhudinal web girders that span between transverse bulkheads. Other transverse components are eliminated, which creates a simple unidirectional structure in the longitudinal direction. The U.S. Navy is currently studying the implementation of an advanced double hull design for surface combatant ships (1). In the commercial sector, product oil earners and tankers have already been built in Japan and Korea (2,3). Some of the reasons for considering double hull ship construction include: a simplified and unidirectional structural system that facilitates automated welding and fabrication techniques; inherent strength for improved ship survivalibility in collision or combay; and fewer areas of discontinuities and complex welded details that could give rise to fatigue and fracture problems. Figure 1 shows the difference between conventional and double hulls of ships.

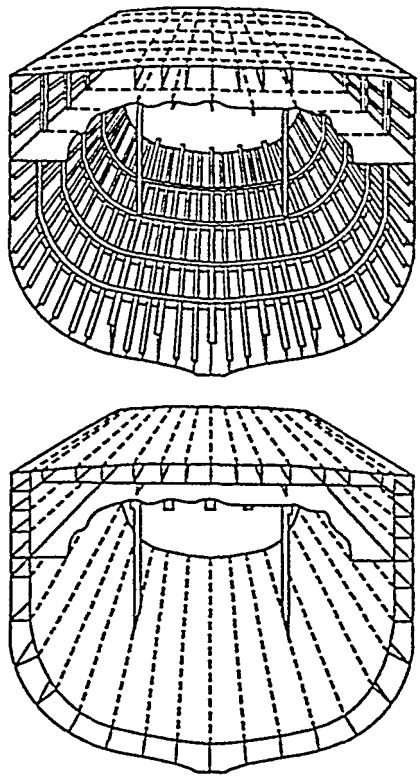

Figure 1: Conventional and advanced double hull designs (1)

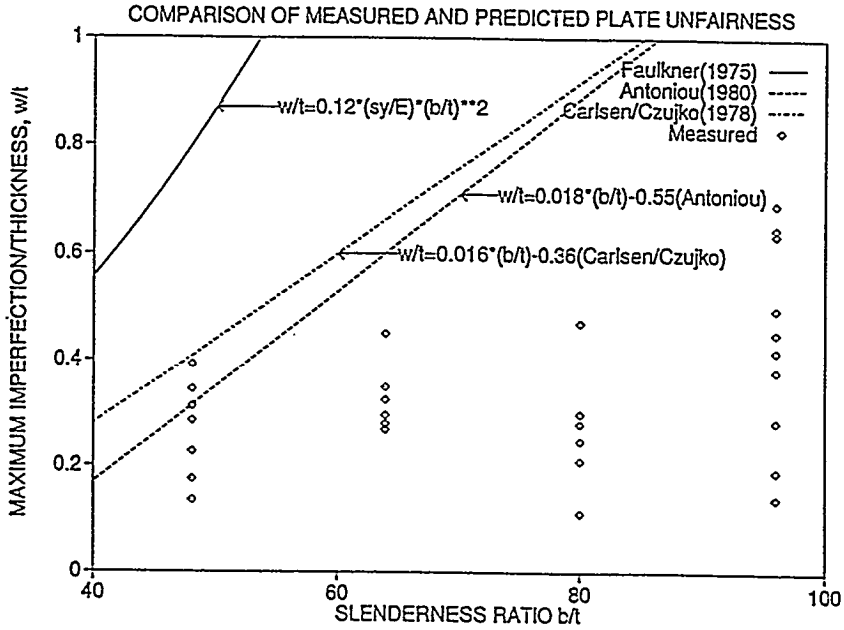

Figure 2: Maximum initial plate deflections

Longitudinal bending of a ship hull gives rise to compressive loads on the cellular components of a double hull. Hence the compressive Stability of these components, in conjunction with lateral hydrostatic presure loads, needs to be considered in design. For practical ranges of plate slenderness ratios, local plate instability will occur first, which in turn affects the stiffness and strength of the cellular beam-columns spanning between transverse bulkheads, in a coupled local-flexural type of overall member failure. It follows, therefore, that the behavior of the component plates must be determined before the overall behavior of the box beam-columns can be studied. Among other factors, local plate behavior is influenced by plate initial imperfections, distortion from the welding process, and welding residual stresses

This paper considers the effects of these two factors on local plate strength and stiffness. The measurement of these imperfections is discussed, and results from the finite element analysis using these measured imperfections are presented.

INITIAL PLATE DEFLECTIONS

Initial plate deflections are a result of various factors, such as the transverse shrinkage of longitudinal edge welds, and handling during the fabrication of the welded structure. Real plates are therefore not perfectly flat. These kinds of deviations from the flat surface (or residual stresses, see following section) suggest a load deflection rather than a buckling problem. In addition to the amplitude of the initial deflection, the longitudinal profile in relation to the plate aspect ratio has an effect on the behavior of the plate. Carlsen and Czujko (4) have shown that the presence of non-elastic buckling modes in the total modal content of the imperfections will always have a strengthening effect on a rectangular plate. However, for design purposes some degree of preferred, elastic buckling mode pattern in the initial deflections must be assumed.

Therefore, in order to assess the effect of initial deflections on plate strength, the initial deflections of each component plate of the multicellular box specimens were measured. The length of the specimens was 182.9 cm (6′) and the cross section consisted of single, double or triple box cells. Square cells were either 457 mm by 457 mm (18″ by 18″) or 914 mm by 914 mm (36″ by 36″), while rectangular cells were 914 mm by 762 mm (36" by 30") or 610 mm by 762 mm (24″ by 30″). The nominal plate thickness was 9.5 mm (3/8″), giving rise to plate width to thickness ratios of 48, 64, 80 and 96. Plate initial deflections of

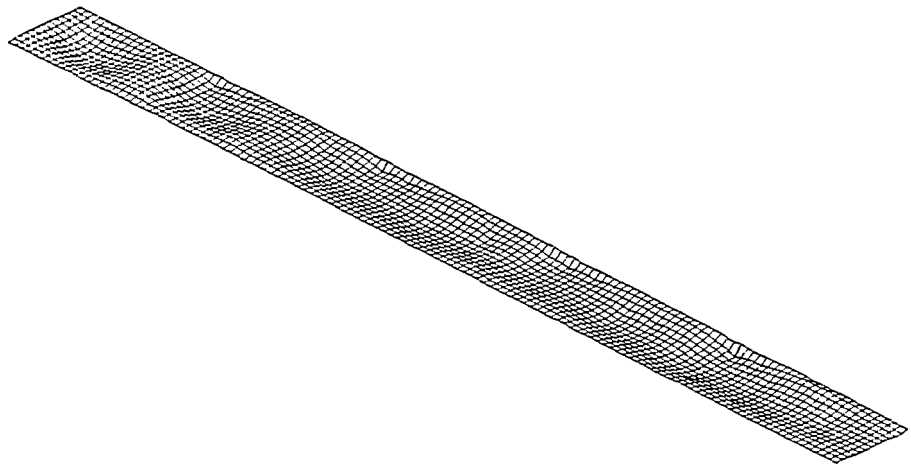

Figure 3: Typical measured out-of-flatness profile for a plate

the test specimens were measured using an aluminum frame with magnetic pads at each end. The function of the pads was to secure the frame to the longitudinal edges of the specimen while the readings were taken. Dial gauges were attached in between the pads and at regular spacings of 228.6 mm or 114.3 mm (9" and 4 1/2"), in order to take readings of the plate surface profile. The reference readings for the dial gauges were first obtained by setting the frame against a flat, milled surface. The measurements commenced at one end of the specimen at the first station, where a series of dial gauge readings were taken across the specimen width. Then the frame was moved to the next station, secured, and readings were taken again. The whole process was repeated until the last station at the other end of the specimen was reached.

The results of the measurements are shown in Figures 2 and 3. In Figure 2, the maximum measured initial deflections as a function of the plate slenderness ratio were plotted and compared to several equations for estimating maximum plate imperfection for a given plate, as proposed by Carlsen and Czujko, (4) Faulkner, (5) and Antoniou (6). The actual measured plate imperfections ranged from 3 to 12 mm (O. 12 to 0.47"), and were below the predictions of the three equations. Faulkner's equation is quadratic and the impetiections increase rapidly with the slenderness ratio. Carlsen and Czujkos', and Antoniou's linear equations show better agreement with the measured values. Measured values were also within the U.S. Navy guidelines for maximun allowable unfairness in ship plating as stipulated in MIL-STD-1689SH - Welding, Fabrication and Inspection of Ship structures.

Figure 3 shows the random surface of one of the component plates of the specimens. Measured profiles were fitted to a double sine series, Equation (1) below, using least squares regression analysis.

$$w = \sum_{i=1}^{m}\sum_{j=1}^{n} A_{ij}\sin\left(\frac{i\pi x}{a}\right)\sin\left(\frac{j\pi y}{b}\right) \quad (1)$$

In general the surface profiles are quite random in nature, although in a few cases, the first longitudinal mode of deflection, i.e., a single longitudinal half wave, predominates. For design purposes it would be impractical to measure actual imperfections, so some conservative procedure, such as the proposed equations mentioned above, would be used.

WELDING RESIDUAL STRESSES

Residual stresses due to welding were measured in a single cell specimen, The stresses were measured using the sectioning method, in conjunction with a 25.4 cm (10") Whittemore

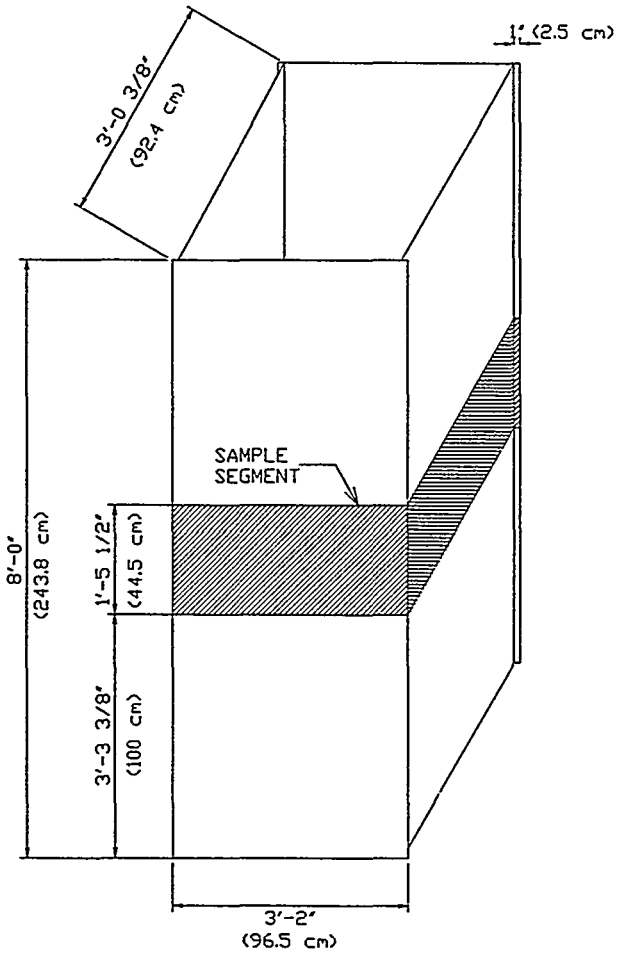

Figure 4: Residual stress test sample segment

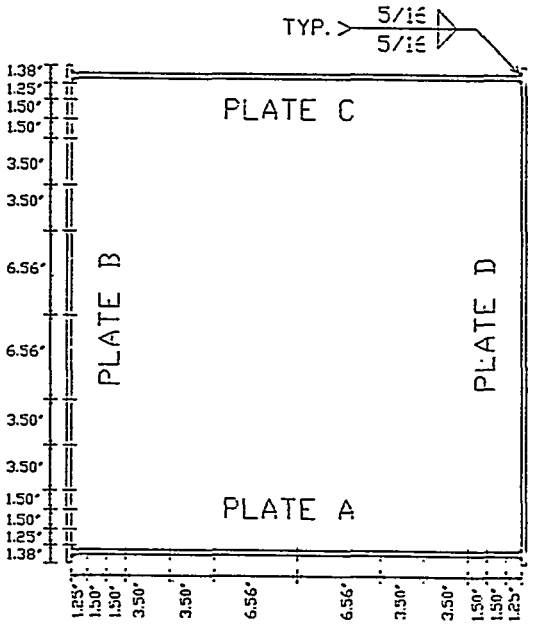

Figure 5: Dissection marks for strips used for residual stress measurements

gauge; the sectioning method was also used in conjunction with strain gauges. A test segment of 44.5 cm (1' 6") in length was removed from the single cell specimen (Figure 4) and used to measure the residual stresses by cutting it into strips. Fillet welds were placed on both sides of the plates to join them (Figure 5). Figure 5 shows the locations where Plates A and B of the segment were cut into strips. Plates C and D had similar cut patterns. In all plates, thinner strips were cut near the welds where a significant gradient in residual stresses was anticipated. The middle strips of each plate were wider, where a more constant residual stress was anticipated. Prior to cutting the segment into strips, a reference strain measurement ε_0 was taken. Strain gauges allowed a direct strain reading from each gauge. The Whittemore gauge, a mechanical device having a 25.4 cm gauge length, required two small holes to be drilled in each strip in order to take strain readings. These holes were drilled at the gauge length of 25.4 cm, centered in the middle of the strip. After placing the instrument and seating it in a pair of drilled holes in a strip, a reference reading was obtained for the strip by averaging three Whittemore measurements. A temperature reference reading was also taken, in order to minimize the effects of any temperature fluctuation of the steel during the measuring period. A liquid coolant was applied to the steel to dissipate any heat created from the cutting process; this way, any secondary residual stresses due to thermal expansion were reduced. Additional strain measurements ε_f were taken after the strips were cut. The difference between these and the reference readings ε_0 provided the residual stresses σ_{res}

$$\sigma_{res} = E(\varepsilon_f - \varepsilon_0) \qquad (2)$$

where E is Young's Modulus, 203.4 GPa (29,500 ksi).

Residual stress measurements were taken on both sides of all four plates. Figure 6 shows the residual stresses measured on the outside of the plates using the Whittemore gauge. The Whittemore gauge results show a nearly constant compressive residual stress distribution over the middle portion of each plate, with a high value of

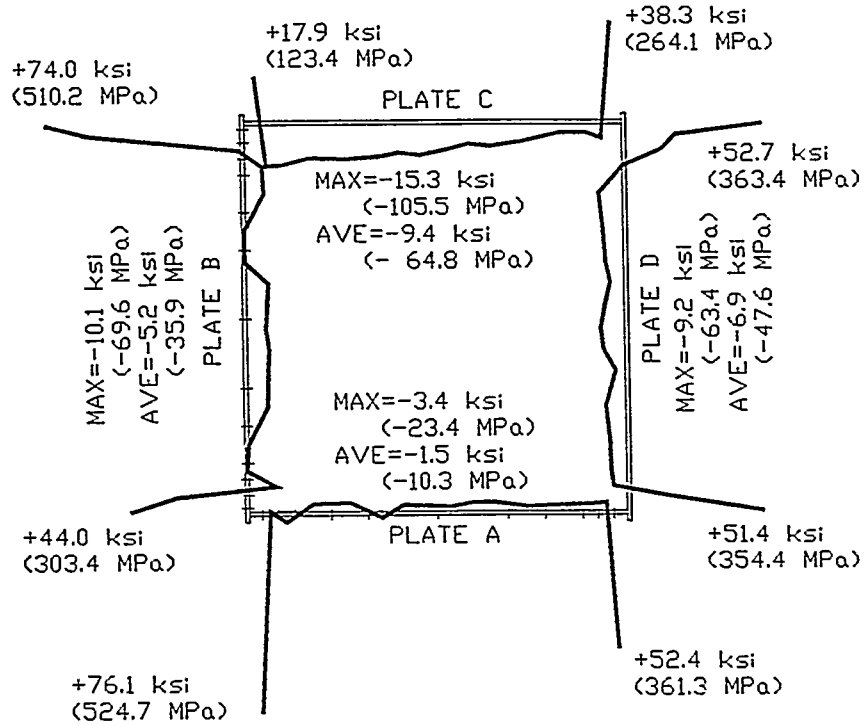

Figure 6: External Surface Longitudinal Residual Stress Distribution-Whittemore Gauge

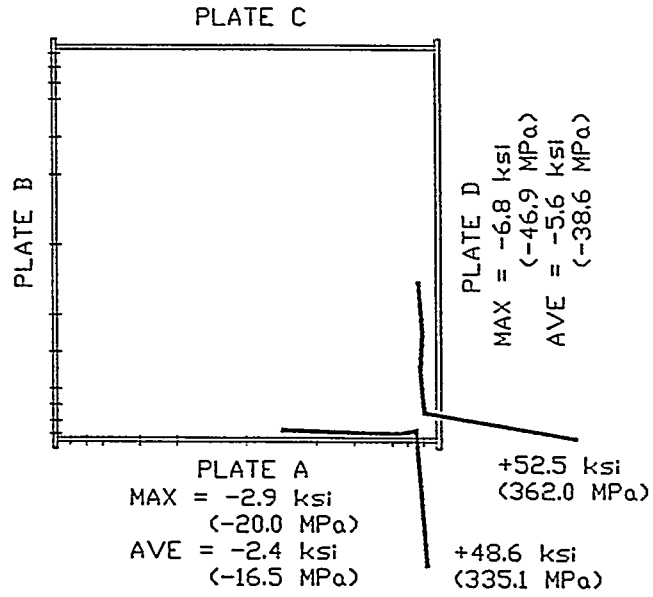

Figure 7: External Surface Longitudinal Residual Stress Distribution-Strain Gauges

tensile residual stress existing at the edges of each plate near the locations of the welds. The residual stress measurements based on the strain gauge reading are shown in Figure 7. Only a portion of plates A and D were strain gauged, as indicated by the location of the results shown in this figure. The strain gauge results agree closely with the Whittemore results, which were taken at similar locations

From the measured residual stresses of each plate, an idealized rectangular pattern of uniform tensile stresses up to yield strength σ_y along the

Plate	Average σ_{rc} MPa	η
A	48.3	3.46
B	52.5	3.74
C	64.7	4.53
D	49.5	3.54

Table I: Values for σ_{rc} and η from the longitudinal residual stress distribution

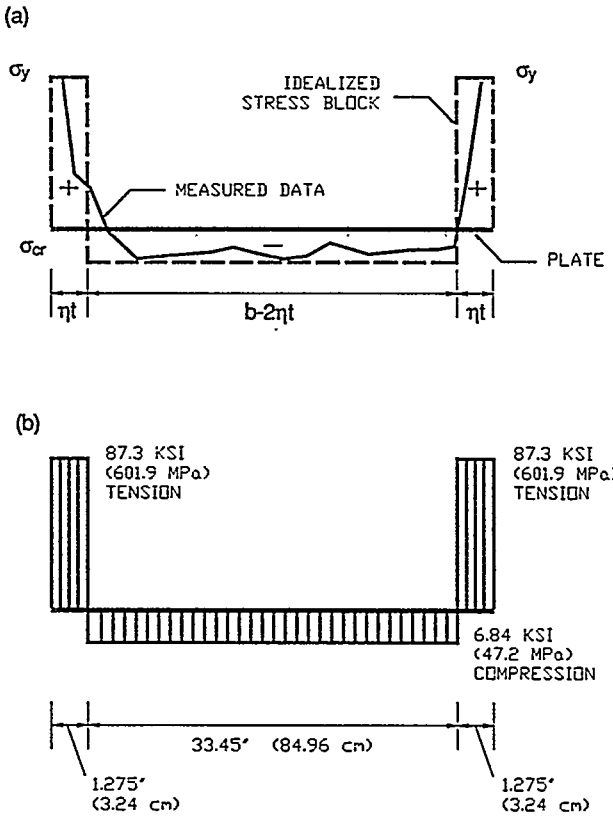

Figure 8: Measured and idealized pattern of longitudinal residual stress, Plate A

longitudinal edges of the plate was calculated, balanced by uniform compressive stress σ_{rc} over the middle strip. For each plate, the compressive stress was averaged over the middle strip of the

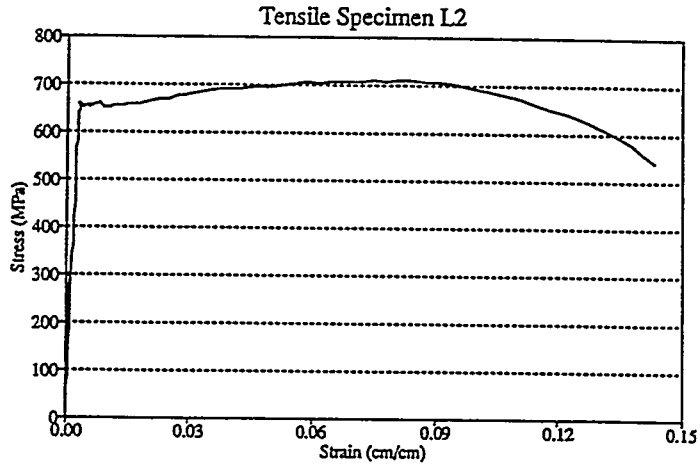

Figure 9: Representative stress strain curve for HSLA-80 tensile coupons

plate. The width of the tensile edge strips was then determined from equilibrium of the residual forces (Figure 8). The computed values of the tensile width parameter, η, was found to vary from 3.46 to 4.53 for the four plates (A, B, C, D) which formed the cell of the residual stress test segment (Table I). Faulkner (5) has recommended values of η from 3.0 to 4.5 for ship plating.

FINITE ELEMENT ANALYSIS

The component plates of the cellular box specimens were analyzed by the finite element (FE) method. The actual measured initial plate deflections, and idealized residual stresses (where η=3.81), were used in the analysis. The plates were modeled with midsurface thin shell elements using a large displacement formulation with material plasticity. Since the actual initial geometric imperfections were used, there was no plate symmetry and hence all the plates were modeled whole. A bilinear kinematic hardening material model was used together with the von Mises yield criterion. Based upon the results of tensile coupon tests, the average yield strength σ_y was equal to 600 MPa (87 ksi) and the strain hardening modulus E_{st} was equal to 1195 MPa (175 ksi). Figure 9 shows a typical stress strain curve from a coupon test performed on HSLA-80 steel.

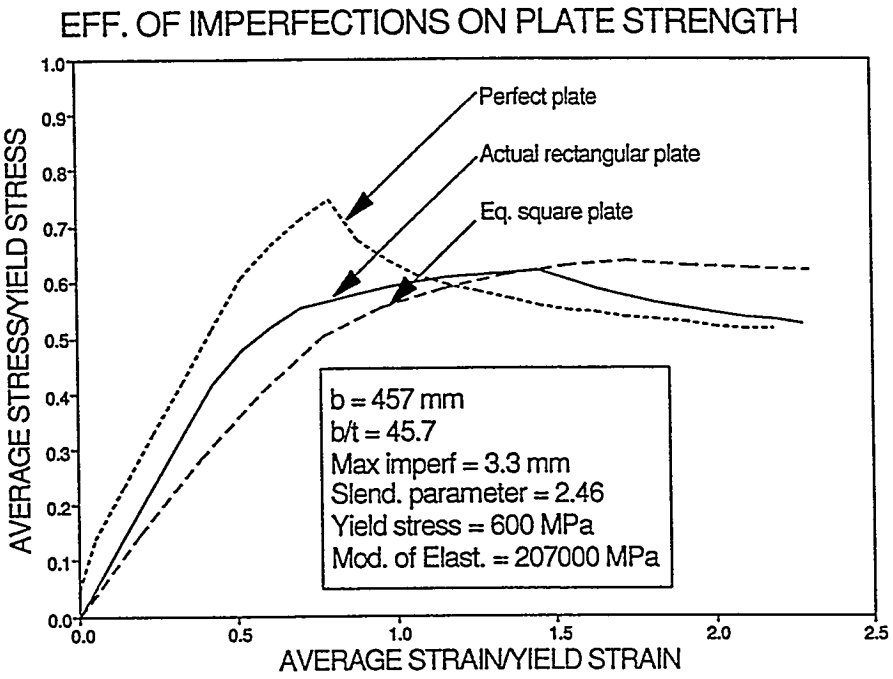

Figure 10: Comparison of load shortening curves, b/t = 45.7

b (mm)	$\frac{b}{t}$	$\frac{\sigma_{re}}{\sigma_y}$ (η=4)	$\frac{w_{max}}{b}$	Maximum Strength		
				Square Plate	'Perfect' Plate	Actual Plate
457	45.7	0.200	0.0072	0.6332	0.7479	0.6174
914	92.5	0.091	0.0072	0.3946	0.5548	0.3825

Table 11 Comparison of maximum plate strengths

The residual stresses were entered directly into each element as initial residual strains. The idealized rectangular pattern was assumed to remain constant over the length of the plate except near the ends, where it linearly decayed to zero over a length of one plate width. Boundary conditions were taken to be simply supported and unrestrained along the longitudinal unloaded edges, and simply supported along the loaded edges. Uniform edge compressive loading was applied by means of prescribed uniform shortenings of the plate from one end, and the total load was obtained from the reactions at the other end.

Figures 10 through 13 show the results of the finite element analyses for two rectangular plates with nominal slenderness ratios b/t equal to 48 and 96, respectively. The nominal aspect ratios a/b are equal to 4 and 2. Figures 10 and 11 compare the load shortening curves for the actual plate, the corresponding "perfect" plate with no residual stresses and initial deflections, and also the corresponding square plate with the same residual stresses and amplitude of initial deflection as the **actual** plate. The imperfection profile for the square plate was taken to be single half waves in both directions. In both plates, it can be seen that plate imperfections have a marked influence on the stiffiess and strength of the plates the influence is also greater for the more slender plate compared to the less slender (stockier) plate. Table 11 lists the maximum strengths of the plates, where it is seen that the percentage strength reduction due to the combined effects of initial deflections and welding residual stresses is about 30% for the slender plate, compared to 1690 for the stockier plate. The imperfections also reduced the gradient of the unloading portion of the curve in the case of the stockier plate, as shown in Figure 10. The load shortening behavior of rectangular plates is often conservatively assumed to be similar to that of an

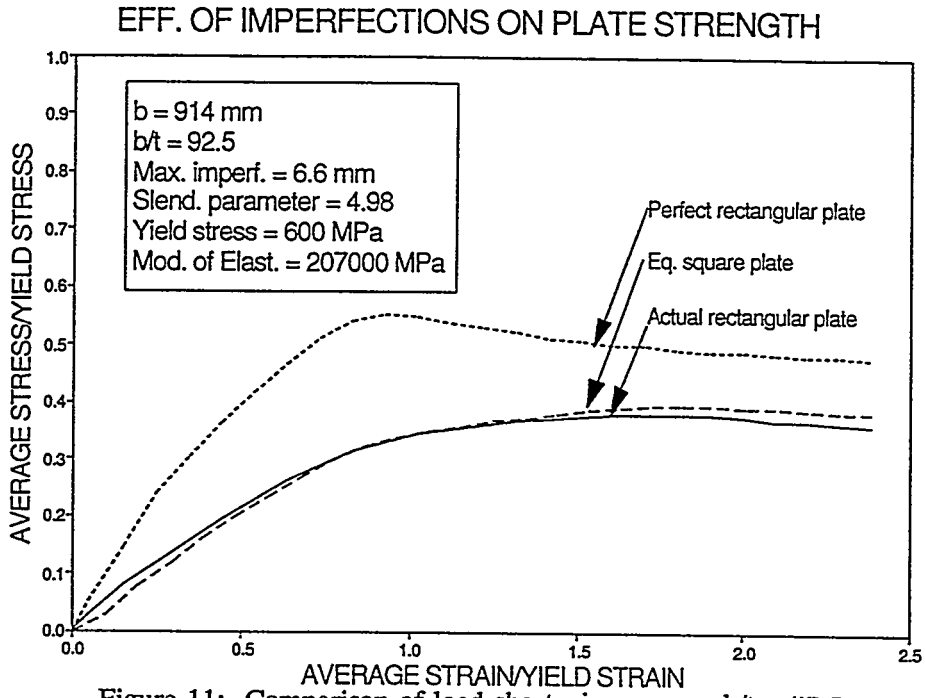

Figure 11: Comparison of load shortening curves, b/t = 92.5

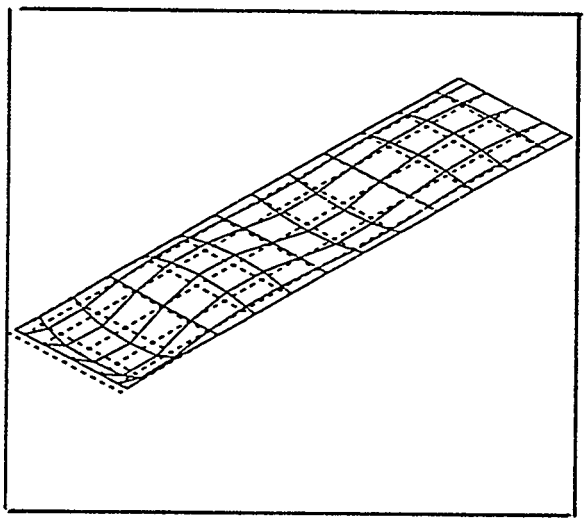

Figure 12: Deflected shape, b/t = 45.7

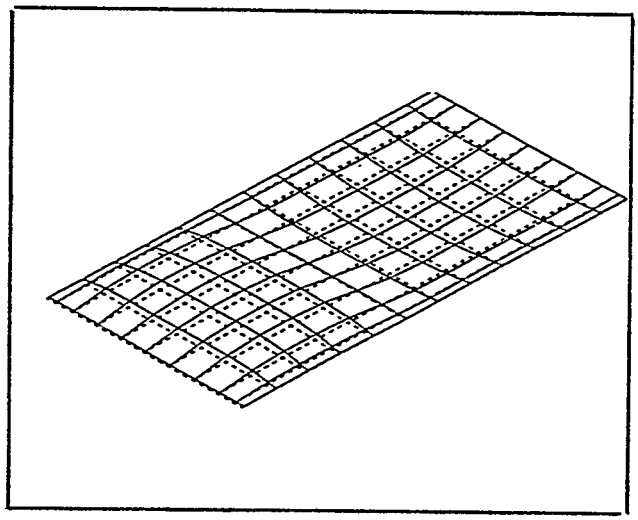

Figure 13: Deflected shape, b/t = 92.5

equivalent square plate. The figures show that the square plate curves are less stiff than the actual rectangular plate curves; peak strengths also do not differ significantly. Figures 12 and 13 show the deformed shape of the plates where the number of half waves formed is clearly seen to be 4 and 2.

The maximum strengths of all the separately analyzed plates of the test specimens (see Table III) are plotted and compared with seeral design equations in Figure 14. The design curves are the Frankland (7) curve which is used by the U.S. Navy, and the Faulkner (5) curve. The latter is plotted for two cases; with and without residual stresses. The elastic buckling curve is also shown for comparison. Frankland's equation gave good predictions at the higher slenderness ratios, but overpredicted somewhat for the stockier plates (b/t=48 and 64). By contrast, all the data points

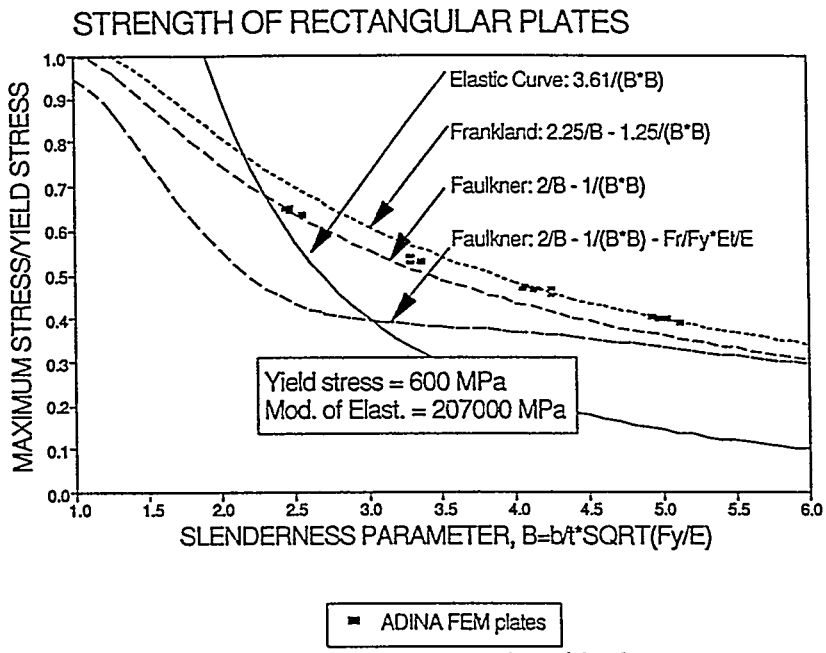

Figure 14: Comparison of FEM plate results with plate design equations

$\beta = \frac{b}{t}\sqrt{\frac{\sigma_{max}}{\sigma_y}}$	$\frac{\sigma_{max}}{\sigma_y}$	$\beta = \frac{b}{t}\sqrt{\frac{\sigma_{max}}{\sigma_y}}$	$\frac{\sigma_{max}}{\sigma_y}$
2.445	0.6490	4.117	0.4625
2.445	0.6494	4.120	0.4640
2.445	0.6496	4.125	0.4715
2.461	0.6461	4.147	0.4704
2.461	0.6528	4.147	0.4711
2.461	0.6426	4.249	0.4549
2.553	0.6334	4.249	0.4676
2.553	0.6345	4.927	0.4050
2.553	0.6371	4.927	0.4002
3.426	0.5283	4.981	0.3983
3.426	0.5417	4.981	0.4000
3.426	0.5400	4.981	0.4002
3.371	0.5298	5.029	0.3984
3.371	0.5339	5.029	0.4008
3.371	0.5322	5.116	0.3876
4.055	0.4690	5.116	0.3906
4.060	0.4758	5.116	0.3922
4.114	0.4711		

Table III: Maximum strengths of rectangular plates by finite element analysis

were above the Faulkner stress-free plate equation. The Faulkner equation for welded plates is seen to give very conservative predictions compared to the finite element results. The results indicate that the Frankland equation is suitable, while the Faulkner equation seems to be the best for estimating plate ultimate strengths.

CONCLUSIONS

Initial imperfections have been shown to affect the behavior of welded plates. The actual measured initial deflections of the welded component plates of a prototype double hull structure were in the range of 3 to 12 mm (0.12 to 0.47"), and within specifications. Measured residual stresses in the component plates of the welded module showed the typical pattern of narrow edge strips of high tension, and a wide middle strip of low, fairly uniform compressive stresses. The maximum strengths of welded plates were reasonably predicted by the Frankland and Faulkner stress-free equations. Results also showed that equivalent square plate load shortening behavior can be used to represent the behavior of the corresponding rectangular plate.

ACKNOWLEDGEMENTS

This work is part of a research project sponsored by the U.S. Navy under a U.S. Navy-

Lehigh University Cooperative Agreement. The support of Mr Jeffrey E. Beach, Head, Surface Ship Structures Division, Naval Surface Warfare Center, David Taylor Model Basin is acknowledged. Thanks are also due to Perry Green, Christopher Schneider and Scott Selleck who helped in some of the measurements. Margaret Kane did the residual stress measurements. The research was earned out at the Center for Advanced Technology for Large Structural Systems, Lehigh University. Dr John W. Fisher is the Director.

REFERENCES

1. Beach, J. E. (1990) "Advanced Surface Ship Technology," ASNE Symposium 1990, pp 89-112.

2. Okamoto, T., Hori, T., Tateishi, M. Rashed, S. M. H., and Miwa, S. (1985) "Strength Evaluation of Novel Unidirectional Girder-System Product Oil Carrier by Reliability Analysis," Trans. SNAME, Vol. 93, pp 1-18.

3. Park, J. K., Kim, D. H., Bong, H. S., Kim, M. S., and Han, S. K. (1992) "Deterministic and Probabilistic Safety Evaluation for a New Double-Hull Tanker with Transverseless System;' Procs. Annual Meeting 1992, SNAME, New York.

4. CarIsen, C. A. and Czujko, J. (1978) "The Specification of Post-Welding Distortion Tolerances for Stiffened Plates in Compression," The Structural Engineer, Vol. 56A, No. 5, pp 133-141.

5. Faulkner, D. (1975) "A Review of Effective Plating for use in the Analysis of Stiffened Plating in Bending and Compression," J. Ship Research, Vol. 19, No. 1, pp 1-17.

6. Antoniou, A. C. (1980) "On the Maximum Deflection of Plating in New Ships," J. Ship Research, Vol. 24, No. 1, pp 31-39.

7. Parlane, A. J. A. (1976) The Determination of Residual Stresses: A Review of Contempormy Techniques, The Welding Institute, Abington Hall, Abington, Cambridge, CBl 6AL, U.K.

8. Frankland, J. M. (1940) "The Strength of Ship Plating under Edge Compression," U.S Experimental Model Basin Report No. 469, Washington, D.C.

Additional copies of this report can be obtained from the
National Shipbuilding Research and Documentation Center:

http://www.nsnet.com/docctr/

Documentation Center
The University of Michigan
Transportation Research Institute
Marine Systems Division
2901 Baxter Road
Ann Arbor, MI 48109-2150

Phone: 734-763-2465
Fax: 734-763-4862
E-mail: Doc.Center@umich.edu